Analysis of Fluorometric Titration Curves

Eugene Novikov,[†,‡] Agnieszka Stobiecka,[†,§] and Noël Boens*[,†]

Department of Chemistry, Katholieke Universiteit Leuven, Celestijnenlaan 200 F, 3001 Heverlee, Belgium, Systems Analysis Department, Belarussian State University, F. Skariny Ave. 4, Minsk 220050, Belarus, and Department of General Food Chemistry, Technical University, Stefanowskiego 4/10, 90-924 Lodz, Poland

Received: January 6, 2000; In Final Form: April 3, 2000

The fluorometric determination of the ground-state dissociation constant K_d of a complex between ligand and titrant with 1:*n* stoichiometry in the presence and absence of excited-state association is discussed. This report extends the results of a previous study (*J. Phys. Chem.* **1994**, *98*, 8585) where a 1:1 complex between ligand and titrant was assumed. For that case, it was demonstrated that adequate experimental design, i.e., by monitoring the fluorescence at the isoemissive point, could eliminate the interference of the excited-state association. In this report we use the direct parametric fit of the fluorometric titration to recover reliable estimates for K_d. It is shown that in the presence of the excited-state association this approach yields the unique value of K_d if a priori knowledge of the excited-state rate constants is available. This method also offers an effective way for discriminating between competitive models (presence and absence of the excited-state association reaction with non 1:1 stoichiometry). The developed algorithms for the direct parametric fit of fluorometric titrations were explored by simulations and were applied to experimental fluorometric titration curves of new Mg^{2+} indicators Thio-H and terThio-H. The importance of the proper choice of experimental conditions— i.e., signal-to-noise ratio, excitation, and emission wavelengths—for the accuracy of the analysis and the quality of discrimination between competitive models is demonstrated.

1. Introduction

Fluorometric titration provides a powerful methodology to determine the ground-state dissociation constant K_d.[1] The advantages of fluorescence over absorption measurements comprise higher sensitivity (because fluorescence is detected vs a dark background) and selectivity (one may avoid the signal from other absorbing molecules). Furthermore, less fluorescent ligand is required in fluorometry than in spectrophotometry to attain a similar sensitivity. Fluorometry generally results in less disturbance of the system and allows less soluble ligands to be used. Fluorescence can also be used with samples of high turbidity. Finally, the geometrical requirements for fluorescence detection are less stringent than for absorption.

However, since the measured fluorescence signal is generally dependent on excited and ground-state parameters (see, e.g., eq 7), one can expect possible interference of the excited-state association on the fluorometric determination of the ground-state dissociation constant K_d. As was shown in ref 1, the presence of an excited-state association between ligand and titrant may yield very complicated fluorometric titration curves. The positions of the inflection points of these curves do not generally contain information that can be directly used for the determination of K_d. In ref 1, we showed that the interference of the excited-state association could be eliminated by proper experimental design, i.e., by monitoring the fluorescence at the isoemissive point. Under this experimental condition, the uncorrupted value of K_d will be obtained from the unique inflection point of the titration curve.

In this paper, we will derive the equations relating the experimental fluorescence signal F to the concentration [M] of the titrant in the presence and absence of the excited-state association with 1:*n* stoichiometry between ligand and titrant. The determination of the position of inflection points (which requires numerical second-order differentiation of noisy fluorescence data) of a titration curve is unreliable, because of statistical noise inherently presented in the measured data and the very limited number of experimental points. Moreover, in the general case, none of the inflection points can be correlated with the true value of K_d. Therefore, in this paper we explore the possibility to determine the correct K_d value via direct parametric fit of the fluorometric titration curve. This curve fitting approach supplies relevant information, which, under certain conditions, can lead to the unique determination of K_d. The direct fit also provides a powerful method for detecting the presence (or absence) of an excited-state association with 1:*n* stoichiometry.

As in ref 1, we use the terminology and methodology of compartmental analysis to describe the steady-state fluorescence.[2]

2. Model

2.1. Steady-State Fluorescence. Consider a dynamic, linear, time-invariant, intermolecular compartmental system, consisting of two distinct types of ground-state species and two corresponding excited-state species, as depicted in Scheme 1 (i.e., two ground-state compartments and two associated excited-state compartments). Ground-state species 1 can undergo a reversible association reaction with M to form ground-state species 2. Scheme 1 assumes a 1:*n* stoichiometry between species 1 and M. It is assumed that only species 1 and 2 absorb light at the excitation wavelength λ_{ex}. $\epsilon_1(\lambda_{ex})$ and $\epsilon_2(\lambda_{ex})$ denote the molar

* To whom all correspondence should be addressed. Tel.: +-32-(0)16-327497. Fax: +-32-(0)16-327990. E-mail: Noel.Boens@chem.kuleuven.ac.be.
[†] Katholieke Universiteit Leuven.
[‡] Belarussian State University.
[§] Technical University.

10.1021/jp000060r CCC: $19.00
Published on Web 05/16/2000

SCHEME 1: Intermolecular System with Stoichiometry 1:*n*

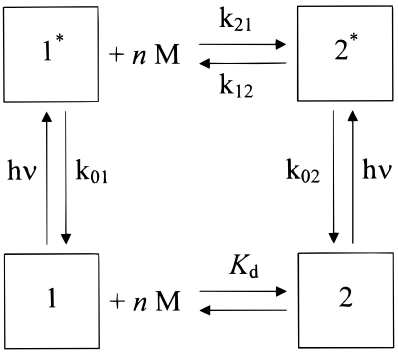

extinction coefficients for species 1 and 2. Excitation by light creates the excited-state species 1* and 2*, which can decay by fluorescence (F) and nonradiative (NR) processes. The composite rate constant for these processes is denoted by k_{0i} ($=k_{F_i} + k_{NR_i}$) for species *i**. The excited-state association reaction of 1* with M is described by the overall $(n + 1)$-order rate constant k_{21}, while k_{12} is the overall first-order rate constant for dissociation of 2* into 1* and *n* M. All rate constants are nonnegative.

Scheme 1 may depict the binding of an ion by a fluorescent ion indicator and the corresponding dissociation of the formed complex. In that case, species 1 represents the free form of the fluorescent ion indicator, species 2 the corresponding bound form, and M the ion. Examples of ion:fluorescent indicator systems for which fluorometric titrations were combined with global compartmental analysis of the time-resolved fluorescence are Ca^{2+}:Fura-2,[3,4] Ca2+:Quin-2,[5] K^+:PBFI,[4,6] Na^+:SBFI,[4] Na^+:SBFO,[7] Mg^{2+}:Mag-fura-2,[8] Ca^{2+}:APTRA-BTC.[9]

It must be emphasized that Scheme 1 represents the *overall* association−dissociation reaction between ligand $1^{(*)}$, titrant M, and complex $2^{(*)}$ with stoichiometry *n*. It is not necessarily indicative for the true detailed mechanism of the reaction, which may consist of consecutive, multiple association (in the forward direction) and dissociation (in the backward direction) steps. If one assumes that the intermediate complexes (with stoichiometry $< n$) are present in concentrations as low as to make only a negligible contribution to the measured fluorescence (in other words, only species 1 and 2 absorb light at the excitation wavelength λ_{ex}), then the steady-state fluorescence signal $F(\lambda_{ex},\lambda_{em},[M])$ measured at emission wavelength λ_{em} due to excitation at λ_{ex} is given by[1,2,10]

$$F(\lambda_{ex},\lambda_{em},[M]) = -\xi(\lambda_{em})\,\mathbf{c}(\lambda_{em})\mathbf{A}^{-1}\mathbf{b}(\lambda_{ex},[M]) \quad (1)$$

where $\xi(\lambda_{em})$ is an instrumental factor, $\mathbf{c}(\lambda_{em})$ is the 1×2 vector of emission weighting factors, **A** is the 2×2 compartmental matrix and $\mathbf{A}^{-1}$ its inverse, and $\mathbf{b}(\lambda_{ex},[M])$ is the 2×1 vector of the zero-time concentrations $[i^*](0)$.

The emission weighting factor $c_i(\lambda_{em})$ of species *i** at λ_{em} is represented as[2]

$$c_i(\lambda_{em}) = k_{F_i}\int_{\Delta\lambda_{em}} \rho_i(\lambda_{em})\,d\lambda_{em} \quad (2)$$

where k_{F_i} is the fluorescence rate constant of species *i**, $\Delta\lambda_{em}$ is the emission wavelength interval round λ_{em} where the fluorescence signal is monitored, and $\rho_i(\lambda_{em})$ is the spectral emission density of species *i** at λ_{em} defined by[2]

$$\rho_i(\lambda_{em}) = F_i(\lambda_{ex},\lambda_{em})/\int_{\text{full emission band}} F_i(\lambda_{ex},\lambda_{em})\,d\lambda_{em} \quad (3)$$

where the integration extends over the whole steady-state fluorescence spectrum F_i of species *i**.

If Beer's law is obeyed and if the absorbance of species *i* is low (<0.1), then the elements $b_i(\lambda_{ex},[M])$ of vector $\mathbf{b}(\lambda_{ex},[M])$ can be approximated as[1]

$$b_i(\lambda_{ex},[M]) \approx 2.3d\epsilon_i(\lambda_{ex})[i]I_0(\lambda_{ex}) \quad (4)$$

where *d* denotes the excitation light path and $I_0(\lambda_{ex})$ is the light flux at λ_{ex} impinging on the sample.

For the system shown in Scheme 1 the compartmental matrix **A** is represented as[1,2]

$$\mathbf{A} = \begin{bmatrix} -(k_{01} + k_{21}[M]^n) & k_{12} \\ k_{21}[M]^n & -(k_{02} + k_{12}) \end{bmatrix} \quad (5)$$

Expressing the ground-state dissociation constant K_d in terms of molalities

$$K_d = \frac{[1][M]^n}{[2]} \quad (6)$$

and substituting eqs 4−6 into eq 1 yields

$$F([M]) = F(\lambda_{ex},\lambda_{em},[M]) = \frac{a_1\epsilon_1K_d + a_2\epsilon_2[M]^n}{K_d + [M]^n}\psi \quad (7)$$

where $\epsilon_i = \epsilon_i(\lambda_{ex})$ for species *i*,

$$\psi(\lambda_{ex},\lambda_{em}) = 2.3dI_0(\lambda_{ex})\,\xi(\lambda_{em}) \quad (8)$$

and $a_i = a_i(\lambda_{em})$ defined by

$$a_1(\lambda_{em}) = \frac{c_1(k_{02} + k_{12}) + c_2k_{21}[M]^n}{k_{01}(k_{02} + k_{12}) + k_{21}[M]^nk_{02}} \quad (9)$$

$$a_2(\lambda_{em}) = \frac{c_2(k_{01} + k_{21}[M]^n) + c_1k_{12}}{k_{01}(k_{02} + k_{12}) + k_{21}[M]^nk_{02}} \quad (10)$$

with $c_i = c_i(\lambda_{em})$ for species *i**. Although in the biophysical literature K_d values are often expressed in molalities (or concentrations), we will consider K_d—a practical (reciprocal) equilibrium constant—as dimensionless, in accordance with the common use in physical chemistry.[11]

2.2. Determination of K_d. *2.2.1. With Excited-State Association Reaction.* Substituting eqs 9 and 10 into eq 7 yields

$$f([M]) = \frac{y_0 + y_1[M]^n + y_2[M]^{2n}}{x_0 + x_1[M]^n + x_2[M]^{2n}} \quad (11)$$

where

$$y_0 = \epsilon_1c_1K_d(k_{02} + k_{12})$$
$$y_1 = \epsilon_1c_2K_dk_{21} + \epsilon_2c_2k_{01} + \epsilon_2c_1k_{12}$$
$$y_2 = \epsilon_2c_2k_{21} \qquad x_0 = K_dk_{01}(k_{02} + k_{12})$$
$$x_1 = K_dk_{21}k_{02} + k_{01}(k_{02} + k_{12}) \qquad x_2 = k_{02}k_{21}$$
$$f([M] = F([M])/\psi \quad (12)$$

The ground-state dissociation constant K_d is one of the roots of the following polynomial

$$x_2K_d^{\,2} - x_1K_d + x_0 = 0 \quad (13)$$

and the other root is expressed as a function of the rate constants as

$$K_d = \frac{k_{01}(k_{02} + k_{12})}{k_{02}k_{21}} \tag{14}$$

If the stoichiometry n is unknown, it should be estimated along with y_k ($k = 0-2$) and x_k ($k = 0-2$). Obviously, full linearization of eq 11 is impossible. The linear functional relationship with respect to the coefficients y_k and x_k,

$$x_0 f([M]) + x_1 f([M])[M]^n + x_2 f([M])[M]^{2n} = y_0 + y_1[M]^n + y_2[M]^{2n} \tag{15}$$

is nonlinearly dependent on n. Although nonlinear estimation of n, y_k ($k = 0-2$) and x_k ($k = 0-2$) is possible (requiring initial guesses for all parameters), a simpler way of perorming the analysis can be suggested. The linear parameters y_k ($k = 0-2$) and x_k ($k = 0-2$) are obtained by linear optimization with the nonlinear parameter n fixed, and the nonlinear parameter n is obtained by nonlinear search when the linear parameters y_k and x_k are fixed. Hence, it becomes an iterative process, where the steps of linear and nonlinear approximation are executed in turn. An initial value is needed only for the parameter n. Since a valid initial value for n can be chosen equal to 1, the whole procedure is rather fast and effective.

If the fluorescence signal is detected at the isoemissive wavelength, where

$$c_1/k_{01} = c_2/k_{02} \tag{16}$$

eq 7 simplifies to

$$f([M]) = \frac{\epsilon_1 c_1 K_d + \epsilon_2 c_1 [M]^n}{K_d + [M]^n} \tag{17}$$

and determination of K_d from eq 17 by linear or nonlinear least-squares minimization methods is straightforward. In that case, the plot of $F([M])$ vs $-\log [M]$ will exhibit a unique inflection point at $[M]^n$ corresponding to K_d.

2.2.2. Without Excited-State Association Reaction. In the absence of reaction in the excited state ($k_{21}[M] \approx 0$), eq 11 simplifies to

$$f([M]) = \frac{y_0 + y_1[M]^n}{x_0 + x_1[M]^n} \tag{18}$$

where

$$y_0 = \epsilon_1 c_1 K_d(k_{02} + k_{12}) \qquad y_1 = \epsilon_2(c_2 k_{01} + c_1 k_{12})$$
$$x_0 = K_d k_{01}(k_{02} + k_{12}) \qquad x_1 = k_{01}(k_{02} + k_{12}) \tag{19}$$

Iterative fitting as in section 2.2.1 yields estimates for the linear parameters y_k ($k = 0, 1$), x_k ($k = 0, 1$), and the nonlinear parameter n. The ground-state dissociation constant K_d is then given by

$$K_d = x_0/x_1 \tag{20}$$

The coefficients a_i (eqs 9 and 10) become independent of [M] so that the steady-state fluorescence signal $F([M])$ is given by[1]

$$F(M) = \frac{[M]^n F_{max} + K_d F_{min}}{K_d + [M]^n} \tag{21}$$

F_{min} corresponds to the steady-state fluorescence signal at very low [M], i.e., the fluorescence of the free ligand 1*, while F_{max} is the steady-state fluorescence signal of the complex 2*. The plot of $F([M])$ vs $-\log [M]$ displays a unique inflection point at $[M]^n$ corresponding to K_d. A reliable K_d value can be estimated by nonlinear fitting of $F([M])$ as a function of [M]: this yields K_d, and additionally n, F_{max}, and F_{min}. Another way of obtaining K_d is via eqs 18−20. Still another way is to rewrite eq 21 in the form of a Hill plot,

$$\log\frac{F([M]) - F_{min}}{F_{max} - F([M])} = n \log [M] - \log K_d \tag{22}$$

To determine K_d and n via a Hill plot, the expression on the left-hand side of eq 22 is plotted vs log [M]. From the slope of this linear graph, a value for n can be derived, while the intersection with the abscissa corresponds to $(\log K_d)/n$. In some cases, it is difficult to obtain reliable values for the extreme values F_{min} and F_{max} from the experimental fluorescence titration. Therefore, the other two methods offer alternatives for the determination of K_d and n.

3. Computer-Generated Fluorometric Titration Curves

The considered algorithms for the analysis of fluorometric titration curves were explored by means of simulations. The fluorometric titration curves were numerically generated according to eqs 11 and 18 at 10 different concentrations (0.5, 1.5, 3.2, 11, and 69 mM, 0.137, 0.737, 1.02, 2.02, and 4.03 M). The values of the system parameters were chosen to mimic the fluorescent K^+ indicator PBFI:[6] $k_{01} = 1.1$ ns^{-1}, $k_{02} = 1.8$ ns^{-1}, $k_{12} = 1.37$ ns^{-1}, $k_{21} = 0.27$ M^{-1} ns^{-1}, $K_d = 6.62 \times 10^{-3}$, $\epsilon_1 = 28\,000$ M^{-1} cm^{-1}, and $\epsilon_2 = 37\,300$ M^{-1} cm^{-1}. Two combinations of the relative emission weighting factors [$c_1^* = c_1/(c_1 + c_2)$, $c_2^* = c_2/(c_1 + c_2)$] were used: $c_1^* = 0.37$ ($c_2^* = 0.63$) and $c_1^* = 0.63$ ($c_2^* = 0.37$). Statistical noise, added to the true fluorescence titration curve, was described by Gaussian statistics; i.e., the value of a fluorescence data point of the titration curve at each concentration is a Gaussian random value, with a mean equal to the exact value for this concentration and a standard deviation defined by

$$\sigma\{f([M]_i)\} = f([M]_i)/\Theta \tag{23}$$

where Θ is the signal-to-noise ratio. Three levels of signal-to-noise ratio Θ were used: 1000, 500, and 100. Fitting was performed in two steps: a linear least-squares algorithm generated initial guesses for the parameters and subsequently the iterative nonlinear least-squares optimization procedure provided the final estimates. Although the fit yields all coefficients x_k, we shall describe only the estimates of the ground-state dissociation constant K_d (and the stoichiometry n). In the model without excited-state association given by eq 18 (we will refer further to it as **model I**) only one value for K_d is recovered, whereas the model with excited-state association given by eq 11 (**model II**) produces two values [roots of the quadratic eq 13]. For each set of system parameters, 100 simulated titration curves were generated, each one with a different realization of statistical noise. The system parameters were estimated for the 100 computer-generated titration curves, and the estimates were stored for the calculation of the mean value

TABLE 1: Mean Value (M) and Corresponding Standard Deviation (σ) of the Estimated Values of K_d by Direct Parametric Fit of the Fluorometric Titration Curves Synthesized According to Models I (A) and II (B)[a]

			$c_1^* = 0.37$; $c_2^* = 0.63$			$c_1^* = 0.63$; $c_2^* = 0.37$		
			Θ			Θ		
fitting model	estimator	true value	1000	500	100	1000	500	100
			A. Model I					
I	$10^3 M\{K_d\}$	6.62	6.62	6.63	6.76	6.62	6.62	6.62
	$\sigma\{K_d\}$		0.10	0.20	1.11	0.045	0.089	0.44
$\chi^2_I(6)/\chi^2_{II}(4)$	F statistics	[0.22; 6.16]	2.51	2.47	2.46	2.44	2.44	2.44
			B. Model II					
II	$10^3 M\{K_d\}$	6.62	6.62	6.61	6.78	6.60	6.61	7.59
	$\sigma\{K_d\}$		0.012	0.022	0.12	0.21	0.42	4.37
	$M\{K_d\}$	7.17	8.92	8.79	9.81	7.14	7.15	9.77
	$\sigma\{K_d\}$		5.49	8.71	20.17	0.49	0.97	7.01
I	$M\{K_d\}$		6.86	6.87	6.91	0.092	0.092	0.10
	$\sigma\{K_d\}$		0.011	0.022	0.12	0.0025	0.0051	0.026
$\chi^2_I(6)/\chi^2_{II}(4)$	F statistics	[0.22; 6.16]	12.5	4.65	2.19	5445	1359	53

[a] The following values of the system parameters were used: $k_{01} = 1.1$ ns^{-1}, $k_{02} = 1.8$ ns^{-1}, $k_{12} = 1.37$ ns^{-1}, $k_{21} = 0.27$ M^{-1} ns^{-1}, $\epsilon_1 = 28\,000$ M^{-1} cm^{-1}, $\epsilon_2 = 37\,300$ M^{-1} cm^{-1}, $K_d = 6.62 \times 10^{-3}$. In all simulations the stoichiometry n was 1; in the fitting the value of n was kept fixed at 1. The values of the F statistics are given at the 95% confidence level. Model I: without excited-state association. Model II: with excited-state association.

$$\mathrm{M}\{K_d\} = \sum_{j=0}^{100} {}^{j}K_d/100 \tag{24}$$

and of the variance

$$\sigma^2\{K_d\} = \sum_{j=0}^{100} {}^{j}K_d{}^2/100 - M\{K_d\}^2 \tag{25}$$

where ${}^{j}K_d$ is the estimator of K_d obtained in run j. The goodness of fit was judged by the χ^2 criterion:

$$\chi^2(\nu) = \frac{1}{\nu}\sum_{i=1}^{10}\left\{\Theta\frac{f^S([\mathrm{M}]_i) - f^E([\mathrm{M}]_i)}{f^S([\mathrm{M}]_i)}\right\}^2 \tag{26}$$

where $f^S([\mathrm{M}]_i)$ and $f^E([\mathrm{M}]_i)$ are, respectively, the simulated (true) and estimated titration data points at $[\mathrm{M}]_i$, ν is the number of degrees of freedom, equal to (10 − number of estimated parameters − 1).

To test whether the two different models give the same goodness of fit (defined by χ^2 criterion) we use F statistics.[12] If the ratio of χ^2 values for two competitive models is higher or lower than the value defined by F statistics at a certain confidence level and a given numbers of degrees of freedom, the model that yields the fit with the higher χ^2 value should be rejected. Otherwise, the two models are indistinguishable within the given statistical noise. In the tests, we apply F statistics at the 95% confidence level.

In the first set of simulation experiments we assume a 1:1 stoichiometry between species 1 and M; in the fitting procedure the value of the stoichiometry n was kept fixed at 1. The results are presented in Table 1.

In the first experiment (Table 1A), titration curves were generated according to model I (without excited-state association) and fitted by two models: by the same model I and by model II (with excited-state association). The recovery of K_d by model I is reasonably accurate in all cases, even for the lowest signal-to-noise ratio. Fitting the more complex model II to the data generated according to model I does not yield noticeable improvements in the quality of fit (F statistics is within the 95% tolerance interval). The estimated values of the coefficients x_2 and y_2 in eq 11 are close to zero, implying the absence of excited-state association.

In the second simulation experiment, titration curves were simulated according to model II (with excited-state association) and K_d was estimated via the same model. The results of the fits are presented in Table 1B. The increased number of unknown coefficients ($\nu = 4$), compared to number in the previous experiment ($\nu = 6$), makes the estimation procedure less stable, especially for the cases with the lower signal-to-noise ratio. It was also observed that the accuracy of estimation as well as the discrimination between competitive models was dependent on the relative emission weighting factors. One can see that for $c_1^* = 0.37$, when the signal-to-noise ratio decreases, the value of χ^2 for the fitting by the correct model II (with excited-state association) becomes comparable to the χ^2 value obtained for the simpler model I (without excited-state association): for the signal-to-noise ratios Θ 100 and 500 the values of F statistics are within the theoretical 95% tolerance interval. For $c_1^* = 0.63$, when the association in the excited stated really occurs, the application of the simpler model I leads to considerably higher values of χ^2, even for the cases of the lowest signal-to-noise ratio. This makes the discrimination between the competitive models straightforward.

In the second set of simulation experiments (Table 2) we consider systems with 1:2 stoichiometry and $c_1^* = 0.63$.

For model I (without excited-state association) the estimation of the ground-state dissociation constant and stoichiometry (n) is rather stable (Table 2A). When the titration curves simulated according to model I are fitted by the model incorporating excited-state association (model II) but with the stoichiometry fixed to 1, roots of the quadratic eq 13 become complex. The latter observation leads to the direct discrimination between these two models despite the fact that the χ^2 criterion does not show a clear difference.

In the second simulation experiment according to model II (Table 2B), n and K_d were first estimated by the correct model. Table 2B demonstrates that any attempts to fit the fluorometric titration data of the system with excited-state association and 1:2 stoichiometry by a simpler model (freely adjustable stoichiometry n and no excited-state association) fail.

To summarize, the direct parametric fit leads to a clear discrimination between competitive models and an accurate estimation of parameters, if certain experimental conditions (signal-to-noise ratio Θ, the properly chosen range of concentrations [M], the excitation and emission wavelengths) are fulfilled.

TABLE 2: Mean Value (*M*) and Corresponding Standard Deviation (σ) of the Estimated Values of K_d and *n* by Direct Parametric Fit of the Fluorometric Titration Curves Synthesized According to Models I (A) and II (B)[a]

			Θ		
fitting model	estimator	true value	1000	500	100
		A. Model I			
I	$M\{n\}$	2	2.00	2.00	2.01
(initial guess	$\sigma\{n\}$		0.012	0.024	0.12
for *n* is 1)	$10^3M\{K_d\}$	6.62	6.61	6.60	6.68
	$\sigma\{K_d\}$		0.19	0.38	1.89
II (*n* fixed at 1)			complex roots		
$\chi^2_I(5)/\chi^2_{II}(3)$	*F* statistics	[0.18; 9.01]	0.83	0.97	1.10
		B. Model II			
II	$M\{n\}$	2	2.00	1.99	2.31
(initial guess	$\sigma\{n\}$		0.040	0.14	1.19
for *n* is 1)	$10^3M\{K_d\}$	6.62	6.60	7.69	15.51
	$\sigma\{K_d\}$		0.61	7.64	16.91
	$M\{K_d\}$	7.17	7.17	7.26	8.30
	$\sigma\{K_d\}$		0.16	0.70	2.65
$\chi^2_I(5)/\chi^2_{II}(3)$	*F* statistics	[0.18; 9.01]	2339	576	22.44

[a] The following values of the system parameters were used: $k_{01} = 1.1$ ns^{-1}, $k_{02} = 1.8$ ns^{-1}, $k_{12} = 1.37$ ns^{-1}, $k_{21} = 0.27$ M^{-1} ns^{-1}, $\epsilon_1 = 28\,000$ M^{-1} cm^{-1}, $\epsilon_2 = 37\,300$ M^{-1} cm^{-1}, $c_1^* = 0.63$ ($c_2^* = 0.37$), $K_d = 6.62 \times 10^{-3}$. In all simulations the stoichiometry *n* was 2. The values of the *F* statistics are given at the 95% confidence level. Model I: without excited-state association. Model II: with excited-state association.

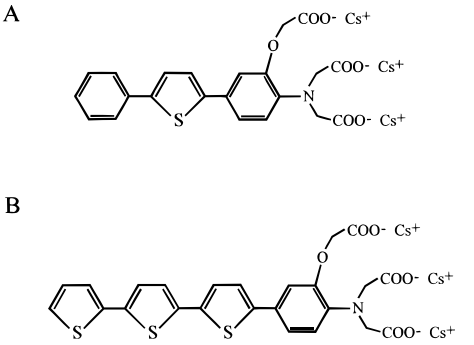

Figure 1. Molecular structures of cesium salts of (A) Thio-H and (B) terThio-H.

In general, there is a straightforward dependence of the quality of parameter estimation on the signal-to-noise ratio Θ and the number of experimental points, but establishing the optimal range of concentrations as well as the choice of excitation and emission wavelengths requires careful experimental design.

4. Experimental Fluorometric Titration Curves

4.1. Materials and Methods. *4.1.1. Materials.* The syntheses of the new Mg^{2+} indicators Thio-H and terThio-H will be described elsewhere.

Cesium salts of Thio-H and terThio-H (see Figure 1) were prepared from the corresponding methyl esters according to the procedure described by Minta and Tsien.[13] A sample of the trimethyl ester of Thio-H or terThio-H was mixed with 10 equiv of anhydrous cesium hydroxide in methanol. The solution was stirred and heated to reflux under argon for 15 h. The purity of the product was checked with analytical thin-layer chromatography using silica plates (Merck). After evaporation of methanol, the product was dissolved in Milli-Q water and was used as such for further measurements. Comparison of the UV spectra of the esters in methanol and the cesium salts in water indicates that the fluorophore structure remains unaltered.

EGTA (ethylene glycol bis(β-aminoethyl ether)-*N*,*N*,*N*′,*N*′-tetraacetic acid) was purchased from Sigma (Bornem, Belgium), MOPS (3-(*N*-morpholino)propanesulfonic acid) was obtained from Fluka (Bornem, Belgium), and $MgCl_2 \cdot 6H_2O$ and KCl were supplied by Aldrich (Bornem, Belgium). All products were used as received.

Values for K_d of the Mg^{2+} complexes of Thio-H and terThio-H were determined in buffered solutions prepared according to the procedure described by Tsien[14,15] and contained (in mM): 100 KCl, 10 MOPS, and 10 EGTA (total concentration). Solutions of MOPS and NaOH were used to obtain the physiological pH of 7.2. Free Mg^{2+} concentrations were calculated using the "Chelator" program[16] and were experimentally obtained by Mg^{2+}/EGTA buffers.

4.1.2. Instrumentation. The absorption measurements were performed on a Perkin-Elmer Lambda 6 UV/vis spectrophotometer. Fully corrected steady-state fluorescence emission spectra were recorded on a SPEX Fluorolog 212. The concentration of the probe in the sample was about 3.2×10^{-6} and 2.4×10^{-6} M for Thio-H and terThio-H, respectively. The absorbance at the absorption maximum of the probe was kept below 0.1. The fluorescence decay traces were collected by the single-photon timing technique.[17,18] A mode-locked Ti:sapphire laser (Tsunami model 3950D, Spectra Physics) pumped by a continuous wave argon ion laser (Beamlock model 2080A-12, Spectra Physics) delivered an 82 MHz pulse train of 1.2 ps width at 798 nm. The repetion rate was reduced to 8.1 MHz by an acousto-optic modulator pulse selector (model 3980-2, Spectra Physics). The laser light was frequency doubled to 399 nm with a lithium triborate crystal (GWU-FHG, Spectra Physics) and adjusted to linear polarization using a Berek Compensator (model 5540, New Focus). Fluorescence of the excited sample passed in a right-angle configuration through a sheet polarizer set to 55.44° with respect to the incident excitation beam and as detected through a monochromator (American Holographics) by a microchannel plate (MCP, R3809U, Hamamatsu). The resulting MCP output start pulse together with the stop signal from a photodiode (818-BB-21, Newport) was connected to a time-correlated single photon counting PC module (SPC 430, Picoquant GmbH). The instrument response function was determined by measuring the light scattered by a LUDOX solution. All decay traces were collected in 4096 channels with a time increment of 2.4 ps and contained approximately $(10-8) \times 10^3$ peak counts after binning in 512 channels (the time increment per channel was 19.5 ps). All measurements were made at room temperature (20 ± 2 °C).

4.1.3. Data Analysis. The existing general global analysis program[19] based on Marquardt's algorithm[20] was used to obtain estimates of the decay times τ_i ($i = 1, 2$). The fitting parameters were determined by minimizing the global reduced χ_g^2:

$$\chi_g^2 = \sum_l^q \sum_i w_{li}(y_{li}^o - y_{li}^c)^2/\nu \qquad (27)$$

where the index *l* sums over *q* experiments, and the index *i* sums over the appropriate channel limits for each individual experiment. y_{li}^o and y_{li}^c denote respectively the experimentally measured (observed) and fitted (calculated) values corresponding to the *i*th channel of the *l*th experiment. w_{li} is the corresponding statistical weight. ν represents the number of degrees of freedom for the entire multidimensional fluorescence decay surface. χ_g^2 and its corresponding $Z_{\chi_g^2}$ (eq 28) provide numerical goodness-of-fit criteria for the entire fluorescence decay surface

$$Z_{\chi_g^2} = (\chi_g^2 - 1)(^1/_2\nu)^{1/2} \qquad (28)$$

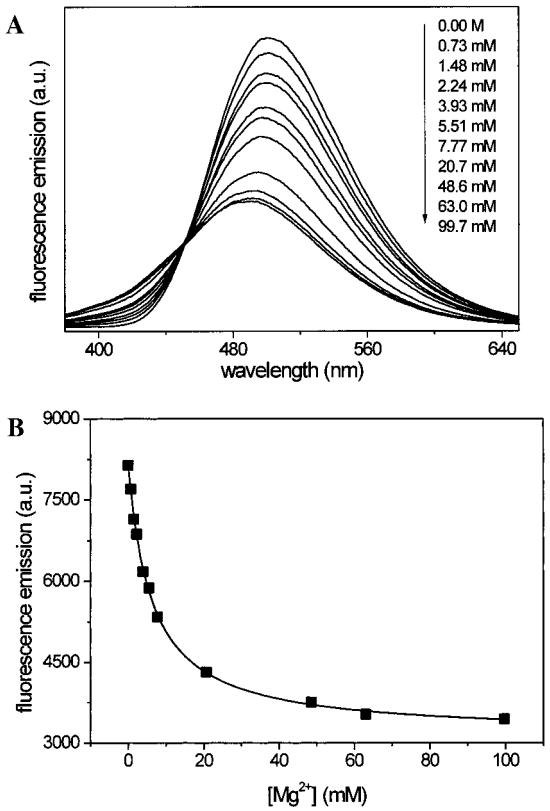

Figure 2. (A) Fluorescence emission spectra of Thio-H as a function of $[Mg^{2+}]$. (B) Nonlinear fit (eq 21) of the fluorometric titration data of Thio-H with n freely adjustable and n fixed at 1: the two fits are indistinguishable (—). The excitation wavelength was set at 364 nm, and the emission was observed at 500 nm.

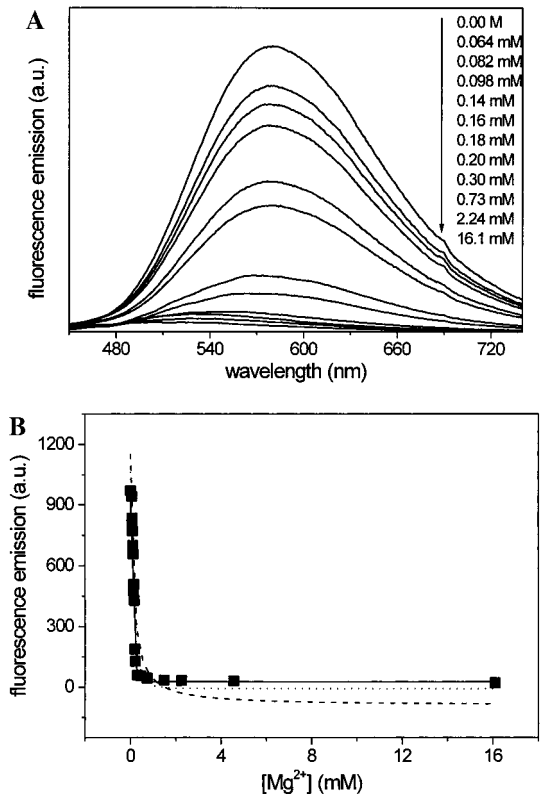

Figure 3. (A) Fluorescence emission spectra of terThio-H as a function of $[Mg^{2+}]$. (B) Nonlinear fit (eq 21) of the fluorometric titration data of terThio-H with n freely adjustable (—), n fixed at 1 (---) and n fixed at 2 (•••). The excitation wavelength was set at 399 nm, and the emission was observed at 580 nm.

Using $Z_{\chi_g^2}$, one can readily compare the goodness-of-fit of analyses with different ν. The additional criteria that were used to judge the quality of the fits are described elsewhere.[18] Standard error estimates were obtained from the parameter covariance matrix available from the analysis. All quoted errors are one standard deviation.

4.2. Results. *4.2.1. Fluorometric Titration of Thio-H.* The fluorescence spectra of Thio-H at various $[Mg^{2+}]$ are shown in Figure 2A. In "0 Mg^{2+}" solutions the spectrum displays a maximum at 500 nm. Increasing the free Mg^{2+} concentration causes a decrease in the peak amplitude (of about 2.4-fold between 0 and 99.7 mM Mg^{2+}) and is accompanied by an increase of the emission intensity at wavelengths below the pseudo-isoemissive point. At elevated levels of Mg^{2+} a minor (i.e., 9 nm) hypsochromic shift can be observed.

The ground-state dissociation constant, K_d, of the Mg^{2+}:Thio-H complex was determined by fitting eq 21 to the steady-state fluorescence data recorded at $\lambda_{em} = 500$ nm due to excitation at $\lambda_{ex} = 364$ nm (Figure 2B). The nonlinear fit (eq 21) with n fixed at 1 yielded a value of $(6.3 \pm 0.2) \times 10^{-3}$ for K_d. This value agrees excellently with K_d and n values estimated according to eq 21 with n freely adjustable: $K_d = (6.3 \pm 0.5) \times 10^{-3}$, and $n = 1.00 \pm 0.05$. Fitting by a more complicated model II (with excited-state association) does not improve the quality of fit: the obtained value of the F statistics is 1.68, which is within the 95% tolerance interval [0.28; 4.15].

4.2.2. Fluorometric Titration of terThio-H. As shown in Figure 3A, the emission spectrum of terThio-H changes significantly upon increasing the Mg^{2+} concentration. The free form of the indicator has a fluorescence maximum at 580 nm. At low magnesium concentrations (0.0 M to 0.16 mM), only a decrease of the emission intensity at the fluorescence maximum is observed. Increasing the free Mg^{2+} concentration above 0.17 mM causes a further decrease in fluorescence intensity and is accompanied by a blue shift of the fluorescence peak. A crossover point at about 480 nm appears.

The results of fitting eq 21 (no excited-state association) to the fluorescence data obtained for different $[Mg^{2+}]$ ranges are compiled in Table 3. When the fluorescence data at all Mg^{2+} concentrations (0.0−16.1 mM) are analyzed, the best fits are found for $n = 3$ and $n = 4$. Fixing n at lower values (1 and 2) yields unacceptable (negative) values for F_{max}. The fit with all parameters freely adjustable indicates that the stoichiometry n is between 3 and 4. For the low $[Mg^{2+}]$ range (0−0.16 mM) acceptable fits could only be obtained when F_{max} was fixed; otherwise, negative values for F_{max} were found. The best fits were again found for high n values ($n = 3$ and 4). The same tendency is observed for the high $[Mg^{2+}]$ range (0.18−16.1 mM in addition to the zero concentration), although the obtained values of F statistics are within the 95% confidence interval. Only the analyses for the total Mg^{2+} concentration range (Table 3A) unambiguously demonstrate non 1:1 stoichiometry.

To check the possibility of the presence of excited-state association, time-resolved fluorescence measurements were performed. Indeed, fluorescence decay times that vary with the Mg^{2+} concentration represent a fingerprint of an excited-state association ($k_{21} \neq 0$).[4] Decay curves of terThio-H at different concentrations of Mg^{2+} ranging from 0.0 M to 0.18 mM were collected at three different emission wavelengths ($\lambda_{em} = 580$, 550, and 470 nm) and a common excitation wavelength ($\lambda_{ex} = 399$ nm).

In the first series of global analyses the decays collected from solutions with identical Mg^{2+} concentrations were described by

TABLE 3: Fitting Eq 21 (without Excited-State Association) to the Experimental Data for terTHIO−H in Different [Mg^{2+}] Ranges[a]

[Mg^{2+}] range	10^6K_d	n	ν	F statistics[e]
A	0.81 ± 0.71[b]	3.5 ± 0.4[b]	14	
	120 ± 37[d]	$n = 1$[d]	15	8.41[d]
	15 ± 3[d]	$n = 2$[d]	15	2.25[d]
	2.2 ± 0.3	$n = 3$	15	0.97
	0.33 ± 0.04	$n = 4$	15	0.94
B[c]	0.06 ± 0.11	4.2 ± 0.8	4	
	74 ± 33	$n = 1$	5	6.76
	7.4 ± 2.3	$n = 2$	5	2.86
	0.8 ± 0.2	$n = 3$	5	1.13
	0.09 ± 0.02	$n = 4$	5	0.67
C	0.28 ± 0.40[b]	3.8 ± 0.8[b]	5	
	30 ± 5	$n = 1$	6	3.80
	5.7 ± 0.6	$n = 2$	6	1.39
	1.10 ± 0.08	$n = 3$	6	0.80
	0.20 ± 0.01	$n = 4$	6	0.72

[a] Key: (A) 0−16.1 mM (total range); (B) 0−0.16 mM (low concentration range); (C) 0.18−16.1 mM (high concentration range) + zero concentration. Number of experimental points: (A) 19; (B) 8; (C) 10. 95% confidence intervals for F statistics: (A) [0.41; 2.46]; (B) [0.19; 6.25]; (C) [0.23; 4.95]. [b] F_{min}, F_{max}, K_d, and n freely adjustable. [c] F_{max} fixed in the fitting, otherwise negative values for F_{max} are found. F_{min} and K_d freely adjustable. [d] Negative value for F_{max} is found. [e] F statistics is calculated as the ratio of unweighted χ^2 with fixed and freely adjustable n: $\chi_{fixed\,n}^2(\nu)/\chi_{free}^2(\nu)$.

TABLE 4: Globally Estimated Decay Times of terThio-H at Different Mg^{2+} Concentrations[a]

[Mg^{2+}] (mM)	τ_1 (ns)	τ_2 (ns)	∂ [b]	χ_g^2	$Z_{\chi_g^2}$
no added Mg^{2+}	0.304 ± 0.002	0.954 ± 0.002	+0.33	1.037	0.827
0.064	0.325 ± 0.004	0.951 ± 0.002	+0.38	1.046	1.029
0.098	0.322 ± 0.002	0.959 ± 0.002	+0.35	1.063	1.425
0.140	0.301 ± 0.002	0.975 ± 0.002	+0.33	1.067	1.518
0.160	0.307 ± 0.002	0.979 ± 0.002	+0.32	1.098	2.206
0.180	0.278 ± 0.005	0.996 ± 0.003	+0.49	1.110	2.469

[a] The number of fluorescence decays analyzed together at each [Mg^{2+}] is 3. [b] Correlation coefficient of the linked parameters τ_1 and τ_2.

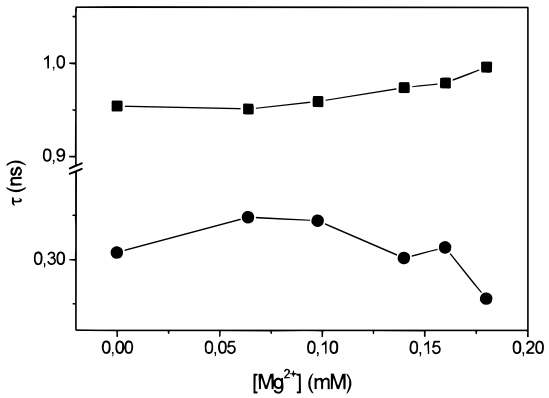

Figure 4. Decay times of terThio-H as a function of [Mg^{2+}].

biexponential functions with the decay times linked over the emission wavelengths at each [Mg^{2+}] (Table 4). The recovered decay times are shown in Figure 4. As is evident from the data compiled in Table 4 and Figure 4, the long decay time τ_2 remains practically independent of [Mg^{2+}] at low cation concentration, i.e., between 0.0 M and 0.098 mM. At the three higher Mg^{2+} concentrations, the long decay time increases slightly. The short decay time τ_1 shows a more erratic behavior with a decrease at higher Mg^{2+} concentrations. To check if the increase of the long decay time τ_2 accompanied by a simultaneous decrease of the short decay time τ_1 at higher Mg^{2+} concentrations can be due to negative correlation between τ_1 and τ_2, the parameter correlation matrix was calculated. Since there is a positive correlation between τ_1 and τ_2 (Table 4), this hypothesis can be rejected.

TABLE 5: Decay Times of terThio-H Estimated by Extended Global Biexponential Analysis

[Mg^{2+}] range (mM)	#[a]	τ_1 (ns)	τ_2 (ns)	χ_g^2	$Z_{\chi_g^2}$
no added Mg^{2+}	3	0.304 ± 0.002	0.954 ± 0.002	1.037	0.827
0.0−0.064	6	0.309 ± 0.002	0.949 ± 0.001	1.052	1.650
0.0−0.098	9	0.315 ± 0.002	0.948 ± 0.001	1.071	2.755
0.0−0.140	12	0.310 ± 0.001	0.961 ± 0.001	1.125	5.641
0.0−0.160	15	0.316 ± 0.001	0.967 ± 0.001	1.244	12.306
0.0−0.180	18	0.313 ± 0.001	0.971 ± 0.001	1.249	13.716

[a] Number of decays analyzed simultaneously in the given [Mg^{2+}] range.

In the second series of global analyses, we subsequently fitted biexponential functions with linked decay times to fluorescence decays measured at various (increasing) Mg^{2+} concentrations. In the final analysis all 18 decay traces were analyzed simultaneously with the decay times linked over 3 different emission wavelengths and over six Mg^{2+} concentrations ranging from 0.0 M to 0.18 mM. As is shown in Table 5, acceptable fits were obtained for the first 9 decays only ($\chi_g^2 = 1.071$, $Z_{\chi_g^2} = 2.755$) yielding values for $\tau_1 = 0.315$ ns and $\tau_2 = 0.948$ ns. Those estimated decay times are in good agreement with the τ_1 and τ_2 values recovered from the global analysis performed before (Table 4) in the [Mg^{2+}] range between 0.0 M and 0.098 mM. Enclosing additional fluorescence decays (more than 9) in the global biexponential analysis increases the values of the goodness-of-fit parameters χ_g^2 and $Z_{\chi_g^2}$, resulting in an unacceptable quality of fits (the other goodness-of-fit parameters also are indicative of unacceptable fits). The extended global biexponential analysis does not give good fits for all decays collected over the whole experimental [Mg^{2+}] range, indicating that the decay times vary with [Mg^{2+}], which implies a nonzero value of k_{21}. In other words, the time-resolved fluorescence data show that the association (binding) reaction in the excited-state cannot be neglected.

Since time-resolved fluorescence measurements imply an ion binding reaction in the excited state, we applied the model given by eq 11 (model II: with excited-state association) to fit the fluorometric titration data. The fluorometric titration curve was experimentally measured for terThio-H at $\lambda_{ex} = 399$ nm and $\lambda_{em} = 580$ nm. As was stated in section 2.2.1, direct parametric fit of the titration curve will give two admissible values of K_d, one of which is the true value and the other is defined as a combination of rate constants (eq 14).

The first direct parametric fits were done by assuming that the stoichiometry n can be fixed at 1 or 2. We compared the fits described by model I (eq 18) and model II (eq 11). For $n = 1$, the fits according to both models were unacceptable, so that this option ($n = 1$) can be rejected immediately. For $n = 2$, the fit by model II is much better than by model I. However, the estimated values of K_d are complex, which leads to the conclusion that the model that takes into account excited-state association with a 1:2 stoichiometry cannot be accepted in this case as well.

Subsequently, we used the same two models (eqs 11 and 18) but with freely adjustable n. Both models recovered higher values of the stoichiometry: 3.1 ± 0.63 for model II and 3.5 ± 0.44 for model I. With model I the recovered value of K_d was $(0.8 \pm 0.7) \times 10^{-6}$. This value is in excellent agreement with that obtained via eq 21 with freely adjustable parameters (see

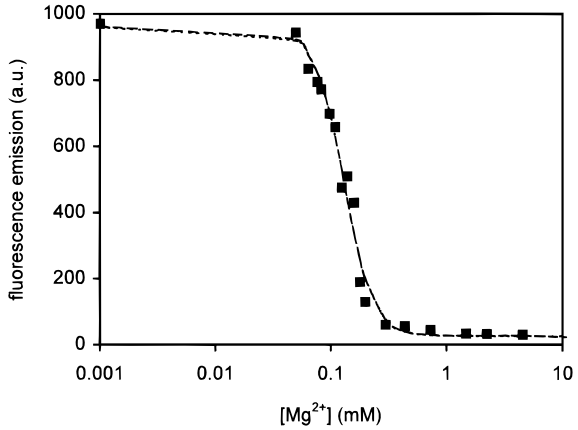

Figure 5. Fit with freely adjustable *n* of the experimental fluorometric titration data of terThio-H according to eq 11 (---) (model with excited-state association) and according to eq 18 (•••) (model without excited-state association). The excitation wavelength was set at 399 nm, and the emission was observed at 580 nm.

Table 3A). In the fit according to model II two values were recovered: $(3 \pm 2) \times 10^{-6}$ and $(5.5 \pm 5.2) \times 10^{-3}$. The fits according to both models are displayed in Figure 5, which shows that the distinction between the two models is fuzzy. This is also supported by the obtained value of the *F* statistics (1.43), which is within the 95% tolerance interval [0.39; 2.64]. On the basis of the performed analyses, one can conclude that the stoichiometry between terThio-H and Mg^{2+} is certainly higher than 2 and most probably between 3 and 4. Comparison of the fits of both competitive models to the fluorometric titration data cannot unambiguously demonstrate the presence (or absence) of excited-state cation binding, but global analysis of the time-resolved fluorescence surface clearly shows its presence. It should be emphasized—as was shown via simulations—that the excited-state association becomes observable in titration curves only under certain experimental conditions. Therefore, to obtain a complete and rigorous characterization of the photophysical processes of an ion indicator, the results of fluorometric titration data analysis and simultaneous time-resolved fluorescence analysis should be combined.

5. Conclusions

In this paper, we have shown that in the presence of excited-state association the direct parametric fit of the titration curve yields the unique value of K_d if a priori knowledge of the excited-state rate constants is available. In the absence of the excited-state association, the direct parametric fit provides the uncorrupted value of K_d. This method also can be used for the discrimination between competitive models (with and without excited-state association, different stoichiometry) used to fit the measured titration curve. We have further demonstrated the importance of the proper choice of experimental conditions (i.e., signal-to-noise ratio, excitation, and emission wavelengths) for the accuracy of the analysis and the quality of discrimination between competitive models.

Acknowledgment. E.N. is grateful to the Research Fund of the K.U. Leuven for a Senior Research Fellowship. A.S. thanks the *Flemish Ministry of Science and Technology* for a postdoctoral fellowship through the *Bilateral Scientific and Technological Cooperation Program* (BIL97/9). Dr. Michael Maus is thanked for assistance with the single-photon timing measurements. N.B. is an *Onderzoeksdirecteur* of the *Fonds voor Wetenschappelijk Onderzoek* (FWO). The financial support of the DWTC (Belgium) through IUAP-4-11 is gratefully acknowledged.

References and Notes

(1) Kowalczyk, A.; Boens, N.; Van den Bergh, V.; De Schryver, F. C. *J. Phys. Chem.* **1994**, *98*, 8585.
(2) Ameloot, M.; Boens, N.; Andriessen, R.; Van den Bergh, V.; De Schryver, F. C. *J. Phys. Chem.* **1991**, *95*, 2041.
(3) Van den Bergh, V.; Boens, N.; De Schryver, F. C.; Ameloot, M.; Steels, P.; Gallay, J.; Vincent, M.; Kowalczyk, A. *Biophys. J.* **1995**, *68*, 1110.
(4) Kowalczyk, A.; Boens, N.; Meuwis, K.; Ameloot, M. *Anal. Biochem.* **1997**, *245*, 28.
(5) Van den Bergh, V.; Boens, N.; De Schryver, F. C.; Gallay, J.; Vincent, M. *Photochem. Photobiol.* **1995**, *61*, 442.
(6) Meuwis, K.; Boens, N.; De Schryver, F. C.; Gallay, J.; Vincent, M. *Biophys. J.* **1995**, *68*, 2469.
(7) Meuwis, K.; Boens, N.; De Schryver, F. C.; Ameloot, M.; Gallay, J.; Vincent, M. *J. Phys. Chem. B* **1998**, *102*, 641.
(8) Meuwis, K.; Boens, N.; Gallay, J.; Vincent, M. *Chem. Phys. Lett.* **1998**, *287*, 412.
(9) Boens, N.; Cielen, E.; Van Werde, K.; De Schryver, F. C. *J. Fluorescence* **1999**, *9*, 103.
(10) Cielen, E.; Tahri, A.; Ver Heyen, K.; Hoornaert, G. J.; De Schryver, F. C.; Boens, N. *J. Chem. Soc., Perkin Trans. 2* **1998**, 1573.
(11) Atkins, P. W. *Physical Chemistry*, 6th ed.; Oxford University Press: Oxford, U.K., 1998.
(12) Hamilton, W. C. *Statistics in Physical Science*; The Ronald Press Co.: New York, 1964.
(13) Minta, A.; Tsien, R. Y. *J. Biol. Chem.* **1989**, *264*, 8171.
(14) Tsien, R. Y. *Biochemistry* **1980**, *19*, 2396.
(15) Tsien, R. Y.; Pozzan, T. *Methods Enzymol.* **1989**, *172*, 230.
(16) Schoenmakers, T. J. M. *Chelator*; Universiteit Nijmegen: Nijmegen, The Netherlands, 1992.
(17) O'Connor, D. V.; Phillips, D. *Time-Correlated Single Photon Counting*; Academic Press: London, 1984.
(18) Boens, N. In *Luminescene Techniques in Chemical and Biochemical Analysis*; Baeyens, W. R. G., De Keukeleire, D., Korkidis, K., Eds.; Marcel Dekker: New York, 1991; p 21.
(19) Boens, N.; Janssens, L. D.; De Schryver, F. C. *Biophys. Chem.* **1989**, *33*, 77.
(20) Marquardt, D. W. *J. Soc. Ind. Appl. Math.* **1963**, *11*, 431.